Syntheses, Characterization and Equilibrium between Mono- and Aqua-bridged Dicobalt(II) Complexes. A Structural Model for Methionine Aminopeptidase

YE, Bao-Hui*(叶保辉)   CHEN, Xiao-Ming(陈小明)
School of Chemistry and Chemical Engineering, Sun Yat-Sen University, Guangzhou, Guangdong 510275, China

A monomeric complex $[Co(Im)_2(O_2CMe)_2]$ (1) and a novel aqua-bridged dimeric complex $[Co_2(\mu\text{-}H_2O)(\mu\text{-}O_2CMe)_2(Im)_4(O_2CMe)_2]$ (2) (Im = imidazole) have been synthesized and characterized. Complexes 1 and 2 coexisted in solution. Pure forms of either complex can be obtained from the same solution by controlling the crystallization conditions. All two complexes possess a carboxylate-Im-cobalt(II) triad system analogous to the carboxylate-histidine-metal triad systems that have been found in many zinc enzymes and cobalt(II)-substituted enzymes. In 2, two Co^{2+} ions are connected by a water molecule in a bridging fashion with $Co\cdots Co$ [0.3687(1) nm], $Co\text{—}OH_2$ [0.2159(3) nm], and $Co\text{-}OH_2\text{-}Co$ [117.2(3)°], in which the water molecule is further stabilized by two intramolecular hydrogen bonds with the oxygens of the terminal monodentate acetate groups with the distance of $O\cdots O$ [0.2609(7) nm]. The terminal monodentate acetate groups display quite abnormal geometry due to the strong "pulling effect" on the carboxylates by intermolecular and intramolecular hydrogen bonds. Complex 2 showed weak antiferromagnetic coupling at low temperature with $g = 2.22$ and $J = -1.60$ cm^{-1}.

Keywords   synthesis, cobalt(II) complex, dinuclear, hydrolase

Introduction

It has been found frequently in hydrolases that two or more metal ions are assembled in very close proximity to the carboxylate side chains of amino acid residues at enzyme active sites to carry out their biological functions.[1] Metals employed in hydrolases include magnesium, manganese, iron, cobalt, nickel and zinc.[1] One kind of hydrolases, the methionine aminopeptidase from *E. coil* (EcMAP)[2] and *Pyrococcus furiosus* (PfMAP)[3] both require two Co^{2+} ions for their activity, whereas their structures are different.

The diverse structures and metals selected at active sites in hydrolases raise such questions as how to orient and activate the substrate molecules including the cosubstrate H_2O, and what type of metal ion to be selected in various hydrolytic processes. In this course, the fixation and activation of water molecule is a crucial step. Coordinate water molecule has been observed in both terminal and bridging binding fashions, and frequently further stabilized and activated through forming

hydrogen bonds with the side chains of amino acid residues at active site in hydrolases.[1] A general two-metal-ion mechanism was proposed for hydrolyzing some of the most important molecules in life such as DNA, RNA, phospholipids and polypeptide.[4] We have synthesized a series of model complexes with the formula $[M_2(\mu\text{-}H_2O)(\mu\text{-}O_2CMe)_2(Im)_4(O_2CMe)_2]$ ($M = Mg^{2+}$, Mn^{2+} and Ni^{2+}).[5] As part of our ongoing study to understand the role of the two metal centers in the overall activity of the hydrolases and to elucidate the mechanism of the hydrolysis reaction, we report herewith the syntheses, characterization and crystal structures of $[Co(Im)_2(O_2CMe)_2]$ (1) and $[Co_2(\mu\text{-}H_2O)(\mu\text{-}O_2CMe)_2(Im)_4(O_2CMe)_2]$ (2).

Experimental

Starting materials were from commercial sources and used without further purification. Deuterium oxide (99.9 %) was purchased from Aldrich. Elemental analyses (C, H and N) were performed on a Perkin-Elmer 240Q Elemental analyzer. The FT-IR spectra were recorded on a Bruker IFS-66 spectrometer using KBr pellet method (4000—400 cm^{-1}). Magnetic susceptibility measurements were carried out on a Quantum Design MPMS SQUID magnetometer at 10 kG (1 T) in the range of 1.8—300 K. Pascal's constants were used to calculate the diamagnetic corrections.

Syntheses of $[Co(Im)_2(O_2CMe)_2]$ (1) *and* $[Co_2(\mu\text{-}H_2O)(\mu\text{-}O_2CMe)_2(Im)_4(O_2CMe)_2]$ (2)

Imidazole (0.136 g, 2.0 mmol) in methanol (5 mL) was added to a methanol solution (10 mL) containing $Co(O_2CMe)_2 \cdot 4H_2O$ (0.249 g, 1.0 mmol). The purple solution was stirred at room temperature for 3 h, and filtered off. (i) Diethyl ether was added to the filtrate. The purple product (1) was obtained, washed by acetone and diethyl ether, and dried overnight *in vacuo*. Yield 0.16 g, 51%. FT-IR (KBr) ν: 1593 (vs), 1573 (vs), 1544 (s), 1418 (s),

1402 (s), 1340 (s), 1265 (m), 1143 (m), 1095 (m), 1073 (s), 767 (s), 684 (m), 666 (s), 662 (s), 618 (m) cm^{-1}. Anal. calcd for $C_{10}H_{14}CoN_4O_4$: C 38.35, H 4.53, N 17.92; found C 38.24, H 4.37, N 17.84. A single crystal suitable for X-ray diffraction was obtained by diffusing diethyl ether into the methanol solution of **1**. (ii) The filtrate was put into a refrigerator for 3 d and the brown crystals (**2**) were obtained, which are suitable for X-ray diffraction study. Yield 53%. FT-IR (KBr) ν: 2326 (w), 1612 (vs), 1538 (s), 1416 (vs), 1331 (m), 1323 (m), 1069 (s), 1009 (m), 941 (m), 905 (m), 827 (m), 754 (m), 657 (vs), 619 (m) cm^{-1}. Anal. calcd for $C_{20}H_{30}Co_2N_8O_9$: C 37.24, H 4.65, N 17.38; found C 37.08, H 4.26, N 17.21. (iii) The filtrate was kept open to the air to evaporate the solvent, and a mixture of brown crystals **2** and purple crystals **1** were obtained. The two crystals with different colors were separated and collected under a microscope and identified by comparing their IR spectra.

Deuterium oxide substitution for the bridging water was prepared by addition of D_2O (1 mL) to **2** (0.1 mmol), and stirring at room temperature for 24 h. Then the powder product was obtained by removing the solvent and dried *in vacuo*.

X-Ray crystallography

Crystal data as well as data collection and refinement for **2** is summarized in Table 1. A single crystal of **2** was mounted on a glass fiber and placed on a Siemens P4 diffractometer equipped with a low-temperature device. Intensity data were obtained by using Mo Kα radiation ($\lambda = 0.071073$ nm) monochromatized from a graphite crystal. Determination of the crystal class, orientation matrix and cell dimensions were performed according to the established procedures. Three standard reflections were monitored after every 150 data measurement, showing only small random variations. The crystal structure was solved by the direct methods and refined with full-matrix least-squares using SHELXTL IRIS program package.[6] Atomic scattering factors were taken from the *International Tables for X-Ray Crystallography*. All the non-hydrogen atoms were refined anisotropically (Table 2). All hydrogen atoms were generated at ideal positions and fixed with isotropic thermal parameters.

Results and discussion

Syntheses

With the aim to synthesize the aqua and carboxylate bridged dinuclear complexes employing monodentate N-donor ligands Im and Bzim, a series of compounds with the formula $[M_2(\mu\text{-}H_2O)(\mu\text{-}O_2CMe)_2(L)_4(O_2CMe)_2]$ (M = Mg^{2+}, Mn^{2+}, Ni^{2+} and Co^{2+}, L = Im and Bzim) has been synthesized in our group.[5] Interestingly, both complexes, mononuclear **1** and dinuclear **2** were obtained from the same reaction of Co$(O_2CMe)_2 \cdot 4H_2O$ with Im in 1:2 ratio in methanol by controlling the crystallization conditions, as illustrated in Eq. (1).

Table 1 Crystallographic and refinement data for complex **2**

Empirical formula	$C_{20}H_{30}Co_2N_8O_9$
M_r	644.4
T (K)	198
Crystal system	Orthorhombic
Space group	*Aba*2
a (nm)	0.8640(1)
b (nm)	1.8980(1)
c (nm)	1.6727(1)
V (nm^3), Z	2.7429(8), 4
D_c (Mg/m^3)	1.560
μ (cm^{-1})	12.71
2θ range for data collection (°)	2.0 to 60.0
Reflections collected	2180
Independent reflections	2072
Observed reflections	1541
GOF	1.17
R	0.0405
R'	0.0417[a]

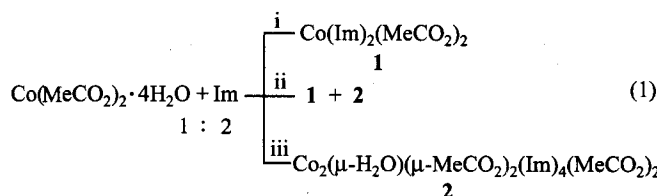[a] $R' = \{\sum[w(|F_o| - |F_c|)^2]/\sum[w|F_o|^2]\}^{1/2}$.

Table 2 Atomic coordinates ($\times 10^4$) and equivalent isotropic displacement coefficients $U_{eq}{}^a$ (nm$^2 \times 10$) for **2**

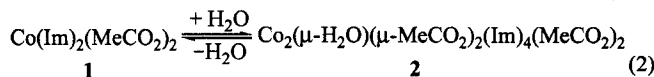| Atom	x	y	z	U_{eq}
Co(1)	1046(1)	847(1)	5000	24(1)
O(1)	0	0	5672(4)	25(2)
O(2)	−946(5)	888(2)	4264(2)	34(1)
O(3)	2147(5)	153(2)	4260(2)	38(1)
C(2)	−1978(6)	468(2)	4026(3)	26(1)
C(21)	−3119(8)	727(3)	3419(5)	52(2)
O(30)	−19(4)	1626(2)	5722(2)	31(1)
C(30)	−1077(6)	1540(2)	6222(3)	31(1)
O(31)	−1643(4)	951(2)	6413(3)	37(1)
C(31)	−1720(8)	2192(3)	6632(4)	43(2)
N(11)	2122(5)	1670(2)	4361(3)	29(1)
C(12)	2263(6)	2334(2)	4598(3)	34(2)
N(13)	3266(6)	2690(2)	4149(3)	35(1)
C(14)	3779(7)	2244(3)	3583(4)	41(2)
C(15)	3081(7)	1615(3)	3712(3)	35(2)
N(21)	2867(5)	830(2)	5865(3)	31(1)
C(22)	4386(6)	851(3)	5736(4)	37(2)
N(23)	5184(5)	869(3)	6427(3)	40(1)
C(24)	4133(7)	854(3)	7038(4)	41(2)
C(25)	2707(6)	834(3)	6682(3)	36(2)

[a] Equivalent isotropic U_{eq} is defined as one third of the trace of the orthogonalized U_{ij} tensor.

Undoubtedly, complexes **1** and **2** coexist in the solution in a chemical equilibrium. When a hydrophobic solvent, such as diethyl ester, was added to the reaction solution, the equilibrium was driven to the formation of **1**. On the other hand, both **1** and **2** were co-crystallized while the reaction solution was open in air under ambient condition to allow the slow evaporation of the solvent. Furthermore, the equilibrium of the

solution was driven to the formation of **2** when the crystallization temperature was lowered to 0 ℃. This may be attributed to the more pronounced decrease of the solubility of **2** than that of **1** when the temperature of the solution was lowered. This observation provides useful insight for the reactivity of **1** with water, since **1** could be viewed as a precursor of **2**. Indeed, **2** may be obtained from the reaction of **1** with water by stirring at room temperature for 5 h, then removing the solvent under reduced pressure (see Eq. (2)). In a reverse reaction, **1** can also be obtained by adding diethyl ether to the methanol solution of **2**. The synthesis of dinuclear zinc complex by the same procedure was not successful. Only a monozinc complex, $[Zn(Im)_2(O_2CMe)_2]$, which is isostructural to **1**, was obtained.[7] This difference between Zn^{2+} and Co^{2+} can be understood by the fact that the former one is difficult to form aqua-bridged complex.[8]

$$Co(MeCO_2)_2 \cdot 4H_2O + Im \underset{1\,:\,2}{\longrightarrow} \begin{cases} \overset{i}{\longrightarrow} \underset{1}{Co(Im)_2(MeCO_2)_2} \\ \overset{ii}{\longrightarrow} 1 + 2 \\ \overset{iii}{\longrightarrow} \underset{2}{Co_2(\mu\text{-}H_2O)(\mu\text{-}MeCO_2)_2(Im)_4(MeCO_2)_2} \end{cases} \quad (1)$$

Crystallization condition: i, add Et_2O; ii, evaporate solvent; iii, lower temperature

$$\underset{1}{Co(Im)_2(MeCO_2)_2} \xrightleftharpoons[-H_2O]{+H_2O} \underset{2}{Co_2(\mu\text{-}H_2O)(\mu\text{-}MeCO_2)_2(Im)_4(MeCO_2)_2} \quad (2)$$

Crystal structure

Complex **2** reveals that the two cobalt ions are assembled by an aqua and two carboxylate bridges as showed in Fig. 1. Each of the two Co^{2+} ions is further coordinated by one additional terminal monodentate carboxylate and two N-donor ligands, forming two equivalent but slightly distorted CoN_2O_4 octahedra joined at their shared vertex by the oxygen atom of the bridging aqua in a face-to-face fashion. The molecule lies on a crystallographically-imposed 2-fold axis passing through the bridging aqua oxygen O(1). Selected bond distances, bond angles and hydrogen bond distances are summarized in Table 3. The hydrogen atoms of the μ-aqua were revealed as the highest residual electron density peak after all other atoms were included in X-ray structure elucidation. The bridging aqua was also identified on the basis of the Co—O (aqua) = 0.2159(3) nm, which falls in the range of 0.2111(5)— 0.218(1) nm observed in $[Co_2(\mu\text{-}H_2O)(\mu\text{-}CO_2R)_2]^{2+}$ cores,[9-14] and is significantly longer than the distances of Co^{2+}—OH in $[Co_2(\mu\text{-}OH)(\mu\text{-}O_2CMe)]^{2+}$ core [0.1934(2) nm],[15] and Co^{2+}—OH [0.2035(12) nm] and Co^{3+}—OH [0.1904(11) nm] in $[Co_2(\mu\text{-}OH)(\mu\text{-}O_2CMe)_2]^{2+}$ core.[16] As expected, the distances of Co—O (aqua) [0.2111(5)— 0.218(1) nm] in aqua bridged dimetallic complexes are considerably longer than those found in terminal binding mode [0.2075(1) nm].[17] The Co—N distances [0.2138(4) and
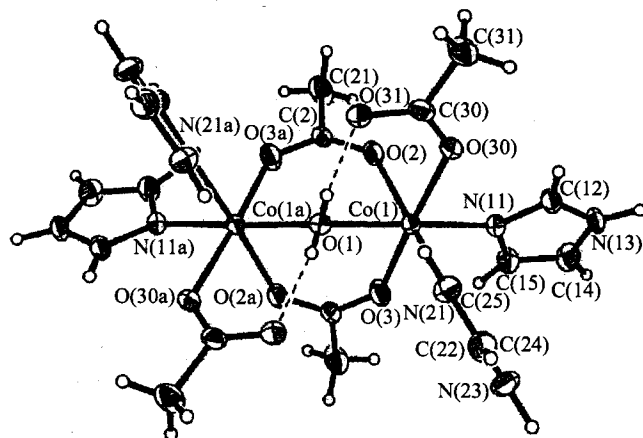

Fig. 1 ORTEP view of **2** showing 40% probability thermal ellipsoids and atom labels as well as the intramolecular hydrogen bonds.

Table 3 Selected bond distances (10^{-1} nm) and angles (°) for **2**

Co(1)—O(1)	2.159(3)	Co(1)—O(2)	2.117(4)
Co(1)—O(3)	2.042(4)	Co(1)—N(11)	2.110(4)
Co(1)—N(21)	2.138(4)	Co(1)—O(30)	2.120(4)
O(1)—Co(1a)	2.159(3)	O(2)—C(2)	1.260(6)
C(2)—O(3a)	1.250(5)	O(30)—C(30)	1.249(7)
C(30)—O(31)	1.261(6)	Co(1)···Co(1a)	3.687(1)
O(1)-Co(1)-O(2)	89.4(1)	O(1)-Co(1)-O(3)	91.8(1)
O(2)-Co(1)-O(3)	92.9(2)	O(1)-Co(1)-N(11)	178.5(1)
O(2)-Co(1)-N(11)	92.1(2)	O(3)-Co(1)-N(11)	88.0(2)
O(1)-Co(1)-N(21)	86.8(2)	O(2)-Co(1)-N(21)	172.9(2)
O(3)-Co(1)-N(21)	93.3(2)	N(11)-Co(1)-N(21)	91.7(2)
O(1)-Co(1)-O(30)	92.3(1)	O(2)-Co(1)-O(30)	87.3(1)
O(3)-Co(1)-O(30)	175.9(1)	N(11)-Co(1)-O(30)	87.9(1)
N(21)-Co(1)-O(30)	86.8(2)	Co(1)-O(1)-Co(1a)	117.2(3)
Co(1)-O(1)-H(1)	96(4)	Co(1a)-O(1)-H(1)	119(4)
H(1)-O(1)-H(1a)	110(8)	Co(1)-O(2)-C(2)	137.3(3)
O(2)-C(2)-C(21)	118.1(4)	O(2)-C(2)-O(3a)	125.5(5)
C(21)-C(2)-O(3a)	116.4(4)	O(30)-C(30)-O(31)	124.7(5)
O(30)-C(30)-C(31)	117.5(4)	O(31)-C(30)-C(31)	117.8(5)
O(1)···O(31)	2.609(7)	N(23)···O(31b)	2.746(8)
N(13)···O(2c)	2.792(8)	H(1)···O(31)	1.89(6)
H(23)···O(31b)	1.69	H(13)···O(2c)	1.83

Symmetry codes: a) $-x, -y, z$; b) $1+x, y, z$; c) $0.5+x, 0.5-y, z$.

0.2110(4) nm] are comparable with those of $[Co(Im)_6]^{2+}$ (0.217 nm),[18] but markedly longer than that in $[Co(Im)_4]^{2+}$ (0.199 nm),[19] and **1** (0.2014 and 0.2019 nm),[7b] indicating that Co—N bond length in a tetrahedral geometry is evidently shorter than that in an octahedral one. The bridging bidentate acetates are found to be markedly asymmetric. The distance of Co(1)—O(2) [0.2117(4) nm] is obviously longer than that of Co(1)—O(3) [0.2042(4) nm]. This can be attributed in part to an additional intermolecular hydrogen bond formed between the oxygen atom of the former

and NH group of Im from the adjacent molecule (O(2)···N(13c)) [0.2792(8) nm] (see Fig. 2), and in part to the ligand *trans* effect.
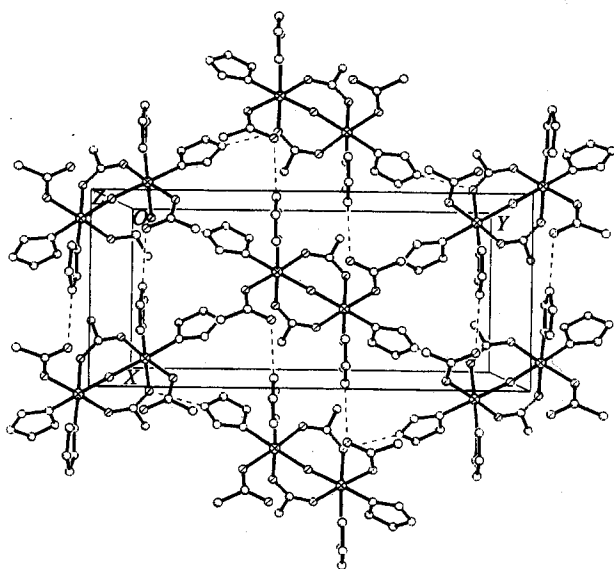

Fig. 2 Packing diagram of **2**, showing the intramolecular and intermolecular hydrogen-bonding network.

The Co···Co distance [0.3687(1) nm] and the Co-O(H₂O)-Co angle [117.2(3)°] are normal in comparison with those found in other [Co₂(μ-H₂O)(μ-CO₂R)₂]²⁺ cores.[9-14] It is well known that the metal-metal distance in the dinuclear active sites is primarily governed by the nature and mode of coordination of the bridging groups. Therefore, it is surprising and interesting that a very short Co···Co distance of 0.29 nm has been observed in the cobalt-dependent EcMAP, in which the two Co(II) ions were regarded as octahedral geometries and bridged through Asp-108 and Glu-235.[2] Though the exact geometries of the Co²⁺ ions can not be identified at 0.24 nm resolution, the presence of the two carboxylate groups in bridge mode is clear. Our synthetic model complex possesses a [Co₂(μ-OH₂)(μ-O₂CMe)₂]²⁺ core, in which the distance of Co···Co (0.36 nm) is obviously too large to well match the 0.29 nm distance in EcMAP. We therefore examined the structural data of dicobalt complexes in literature, and found that it is impossible to bring two Co²⁺ ions at such a short distance of 0.29 nm only through two bridging bidentate carboxylates. From the point of coordination chemistry, the Co···Co distance linked by quadruple triatom-bridge ligands, [Co₂(μ-phCO₂)₄]²⁺, is at 0.283 nm;[20] those linked by triplet bridged ligands, two *syn* bidentate carboxylate and additional monoatomic bridging (H₂O, OH⁻ and ⁻O₂CMe), all fall in the range of 0.34—0.37 nm,[9-14,21] and which linked by double single oxygen-bridged ligands is at 0.315 nm[22] and that linked by a *syn* bidentate carboxylate and a single oxygen bridges, [Co₂(μ-OH)(μ-O₂CMe)]²⁺ is at 0.34 nm.[15] Since the solvent ligands (water and/or hydroxo) have not been observed at 0.24 nm resolution, the active site

structure of EcMAP may be proposed to contain one or two bidentate carboxylate and at least two single oxygen bridges on the basis of taking into account the Co···Co distance (0.29 nm). Indeed, a dicobalt(II) complex with the [Co₂(μ-H₂O)₂(μ-CO₂R)₂]²⁺ core (0.3056 nm) was reported recently.[23]

Acetate ligands display two coordination modes, terminal monodentate and bridging bidentate. A quite intriguing structural feature is noticeable at the terminal carboxylate groups that display an unusual geometry. The distances of C—O (free) 0.1261(6) nm is longer than that of the C—O (coordinated) 0.1249(7) nm. This observation is contrary to the classical geometry of terminal monodentate mode of carboxylate group, in which the distance of C—O (free) is usually shorter than that of C—O (coordinated).[24] A careful examination of the structures leads us to believe that the elongated C—O (free) is the consequence of a strong "pulling effect" on the O (free) atom of the terminal carboxylate arising from two hydrogen bonds (see Fig. 2), an intramolecular one with the bridging aqua [O(1)···O (free), 0.2609(7) nm], and an intermolecular one with the non-coordinating NH group from an adjacent molecule [O (free)···N, 0.2746(8) nm], giving rise to what may be regarded as a "pseudo-bridging" arrangement of the terminal acetate groups.[25]

The significance of the observed framework of H-bonds in the formation and stabilization of **2** can be envisioned by the inspection of Fig. 2, in which the intermolecular packing and H-bonds were displayed. The aqua molecule in a bridging fashion between two cobalt ions is stabilized by the intramolecular H-bonds formed with the terminal carboxylates. This typical H-bond plays a crucial role in fixing and activating the bridging aqua or hydroxide in the process of hydrolysis by dimetalloenzymes. The model compound is genuinely intriguing in that its structure suggests a novel role for these H-bonds in assisting and modulating the production of nucleophilic OH⁻ group, a required reactant for the enzymatic reaction in dimetallic hydrolases. The OH⁻ group can be generated by the deprotonation of the coordinate water that forms an intramolecular hydrogen bond with an ancillary carboxylate side chain of an amino acid. In this process, the carboxylate ligand serves as H-bond acceptor while the bridging aqua serves as the H-bond donor. Interchanges between these tautomers possibly involve the proton transfer processes via the very strong intramolecular H-bonds, displaying an abnormal geometry of carboxylate group and a dramatic downshift of asymmetric O—H stretch of the bridging aqua in IR spectra (see below). The other important structural feature concerning hydrogen bond found in **2** is the carboxylate-Im-metal(II) triad system. Such triad fragment has been found in many zinc hydrolase enzymes and believed to play a crucial role in both structural and mechanistic aspects of enzyme functions.[7b]

IR spectra

The IR spectra of **1** and **2** exhibit very different features.

In other words, IR spectroscopy can be used to identify the monomer **1** from the dimer **2**. First, the symmetric and asymmetric stretching vibrations of carboxylate groups display characteristic bands. There are two $\nu_{as}(CO_2)$ (1593 and 1574 cm^{-1}) and two $\nu_s(CO_2)$ (1419 and 1402 cm^{-1}) peaks in **1**, corresponding to the two different geometries of the coordinating acetate groups. These can be accounted for by the formation of two different types (*syn* and *anti*) hydrogen bonds of carboxylates with Im groups in solid state.[7b] If the hydrogen bonds were considered as a weak bond, the acetate groups can therefore be regarded as two types of bridges between metal ion and hydrogen atom, namely triatomic and monoatomic bridges. Thus the bands at 1593 and 1402 cm^{-1} can be assigned to the stretching modes of the monoatomic acetate bridge, and those at 1574 and 1419 cm^{-1} to the triatomic acetate bridge. Although there are two different types of acetate groups in **2**, the IR spectrum shows only one set of carboxylate vibrations of $\nu_{as}(CO_2)$ at 1612 cm^{-1} and $\nu_s(CO_2)$ at 1416 cm^{-1}, respectively. This observation suggests that the geometries of the two types of carboxylate ligands should be very similar to each other. Indeed, X-ray data revealed that the difference between C(2)—O(2) and C(2)—O(3a) (0.0010 nm) is virtually the same as that between C(30)—O(31) and C(30)—C(30) (0.0012 nm) within the experimental uncertainty. The homology of the two types of carboxylate ligands reflects the effect of H-bond. In addition, a broad band centered at *ca*. 2326 cm^{-1} was observed in the spectrum of **2**, and is attributed to the O—H stretching of the bridging water. The unusual low vibrational frequency of O—H bond is consistent with their involvement in strong H-bonding as revealed also by the X-ray structures. This is also in agreement with the prediction by the classical formula of Bellamy and Owen.[26] Similar phenomena were also observed for aqua-bridged di-Co^{2+} and di-Mn^{2+} complexes.[11,27] When deuterium oxide was used to substitute the water molecule, the typical broad band of O—D stretching vibration was shifted to *ca*. 2303 cm^{-1}. The unusual low ratio of $\nu(O—H)$ to $\nu(O—D)$ is consistent with the systematic observation in organic systems containing strong hydrogen bond, in which the ratio of $\nu(O—H) : \nu(O—D)$ is approaching 1.[28]

Magnetic properties

The temperature-dependent magnetic behavior for powder sample of **2** was collected in the range of 1.9—300 K. The molar paramagnetic susceptibility increases with decreasing temperature and reaches a maximum at 6.0 K, below which the susceptibility starts to decrease rapidly, indicating antiferromagnetic coupling between the two Co^{2+} ions through the aqua bridge. A least-squares fit of the molar susceptibility by the general isotropic exchange Hamiltonian, $H = -2JS_1S_2$, $S_1 = S_2 = 3/2$, produced the best fit with $J = -1.60$, $g = 2.22$ cm^{-1}. The zero-field splitting terms were ignored in the fitting because the coupling was very weak and they would not contribute significantly to the understanding of the behavior of these complexes. The very small negative exchange coupling constant in **2** is consistent with the relatively large Co$\cdots$Co separation and the weak superchange provided by the aqua bridge. The Néel temperature in **2** is comparable to the data from similar complexes.[9,11]

References

1 Wilcox, D. E. *Chem. Rev.* **1996**, *96*, 2435.

2 Roderick, S. L.; Matthews, B. W. *Biochemistry* **1993**, *32*, 3907.

3 Tahirov, T. H.; Oki, H.; Tsukihara, T.; Ogasahara, K.; Yutani, K.; Ogata, K.; Izu, Y.; Tsunasawa, S.; Kato, I. *J. Mol. Biol.* **1998**, *284*, 101.

4 Steitz, T. A.; Steitz, J. A. *Proc. Natl. Acad. Sci. U. S. A.* **1993**, *90*, 6498.

5 (a) Ye, B.-H.; Mak, T.; Williams, I. D.; Li, X.-Y. *Chem. Commun.* **1997**, 1813.
   (b) Schultz, B. E.; Ye, B.-H.; Li, X.-Y; Chan, S. I. *Inorg. Chem.* **1997**, *36*, 2617.
   (c) Ye, B.-H.; Mak, T.; Williams, I. D.; Li, X.-Y. *J. Chem. Soc., Dalton Trans.* **1998**, 1935.

6 Sheldrick, G. M. *SHELXTL-IRIS*, Simens Analytical X-Ray Instruments Inc, German, **1993**.

7 (a) Horrocks, W. D.; Ishley, J. N.; Whittle, R. R. *Inorg. Chem.* **1982**, *21*, 3265.
   (b) Chen, X.-M.; Ye, B.-H.; Xu, Z.-T.; Huang, X.-C. *J. Chem. Soc., Dalton Trans.* **1996**, 3465.

8 Cotton, F. A.; Wilkinson, G. *Advanced Inorganic Chemistry*, 4th edn., John Wiley and Sons, New York, **1980**, p. 768.

9 Turpeinen, U.; Ahgrén, M.; Hämäläinen, R. *Acta Crystallogr.* **1982**, *B38*, 1580.

10 Ahgrén, M.; Hämäläinen, R.; Turpeinen, U. *Finn. Chem. Lett.* **1983**, 125.

11 Turpeinen, U.; Hämäläinen, R.; Reedijk, J. *Polyhedron* **1987**, *6*, 1603.

12 Coucouvanis, D.; Reynolds, R. A. III; Dunham, W. R. *J. Am. Chem. Soc.* **1995**, *117*, 7570.

13 Hagen, K. S.; Lachicotte, R.; Kitaygorodskiy, A.; Elbouadili, A. *Angew. Chem., Int. Ed. Engl.* **1993**, *31*, 1321.

14 Hagen, K. S.; Lachicotte, R.; Kitaygorodskiy, A. *J. Am. Chem. Soc.* **1993**, *115*, 12617.

15 Jaynes, B. S.; Doerrer, L. H.; Liu, S.; Lippard, S. J. *Inorg. Chem.* **1995**, *34*, 5735.

16 Chaudhuri, P.; Querbach, J.; Wieghardt, K.; Nuber, B.; Weiss, J. *J. Chem. Soc., Dalton Trans.* **1990**, 271.

17 Hänggi, G.; Schmalle, H.; Dubler, E. *Acta Crystallogr.* **1992**, *C48*, 1008.

18 Gadet, A.; Soubeyran, O. L. *Acta Crystallogr.* **1974**, *B30*, 716.

19 Gadet, A. *Acta Crystallogr.* **1974**, *B30*, 349.

20 Drew, J.; Hursthouse, M. B.; Thotnton, P.; Welch, A. J. *J. Chem. Soc., Chem. Commun.* **1973**, 52.

21 (a) Catterick, J.; Hursthouse, M. B.; New, D. B.; Thotnton,

P. *J. Chem. Soc., Chem. Commun.* **1974**, 843.

(b) Catterick, J.; Hursthouse, M. B.; New, D. B.; Thotnton, P. *J. Chem. Soc., Dalton Trans.* **1976**, 1634.

22   Hoskins, B. F.; Williams, G. A. *Aust. J. Chem.* **1975**, *28*, 2607.

23   Lee, D.; Huang, P.-L.; Spingler, B.; Lippard, S. J. *Inorg. Chem.* **2002**, *41*, 521.

24   Oldham, C. In *Comprehensive Coordination Chemistry*, Vol. 2, Eds.: Wilkinson, G.; Gillard, R. D.; McCleverty, J. A.;

Pergamon, Oxford, U.K., **1987**, p. 435.

25   Deacon, G. B.; Phillips, R. J. *Coord. Chem. Rev.* **1980**, *33*, 227.

26   Bellamy, L. J.; Owen, A. J. *Spectrochim. Acta, Part A* **1969**, *25*, 329.

27   Yu, S.-B.; Lippard, S. J.; Shweky, I.; Bino, A. *Inorg. Chem.* **1992**, *31*, 3502.

28   Hibbert, F.; Emsley, J. *Adv. Phys. Org. Chem.* **1990**, *26*, 279.

(E0206242   PAN, B. F.; LING, J.)